IUST International Journal of Engineering Science, Vol. **19**, *No.***3**, **2008**, *Page* **7-16**
Chemical & Civil Engineering, Special Issue

DIFFUSION AND REACTION WITHIN A SHAPED NICKEL PEROVSKITE CATALYST

Matin Parvari & Peyman Moradi

Abstract: *In this study, we prepared a $LaNi_{0.3}Al_{0.7}O_3$ perovskite catalyst using a sol-gel related method (with prop ionic acid as a solvent) for use in the methane dry reforming reaction to produce synthesis gas. We defined the catalyst structure on the basis of X-ray diffraction analysis and measurements of the specific surface area and particle size distribution. The mixed oxide structure was shaped into a cylindrical pellet before being measured for its mechanical strength. The shaped perovskite catalyst was then tested in the methane dry reforming reaction to produce synthesis gas at atmospheric pressure. The results are compared with the predictions of a mathematical model that is used to estimate the concentration profile within the pellet. The outlet concentration of the reactants and conversion products calculated by the mathematical model has been consistent with the results obtained by experiments conducted in a fixed bed reactor.*

Keywords: *Nickel, Perovskite, Diffusion, Dry Reforming, Synthesis Gas.*

1. Introduction

The natural gas to liquid fuel process (GTL) is composed of two parts: One is the synthesis gas generation from natural gas (methane), and the other is synthesis gas conversion to liquid fuels. During the last several years, there has been renewed interest in the catalytic reforming of methane with carbon dioxide, rather than steam, for the production of synthesis gas because synthesis gas with lower H2/CO can be produced from methane by CO2 reforming which is suitable for Fischer-Tropsch plants. Another advantage is the effective use of CO2, a well known green house gas, as a carbon resource.

Also, methane reforming with carbon dioxide has been studied for viability in chemical energy transmission systems[1].

$$CH4 + CO2 \rightarrow 2CO + 2H2,\ H2/CO = 1\ (CO2\ refor\min g)$$

$$CH4 + H2O \rightarrow CO + 3H2,\ H2/CO = 3(Steam\ refor\min g)$$

$$nCO + 2nH2 \rightarrow -(CH2)n- + nH2O,\ H2/CO = 2$$

(Fischer-Tropsch)

Mathematical modeling of the diffusion and reaction process is a strong tool for design and research. Unfortunately, models for the devices that are most often used in industry (e.g., fixed bed reactors) are highly complex. Mathematically, the models are partial differential equations (boundary-value problems) that are difficult and/or take a long time to solve. The commonly applied effectiveness factor concept reduces the equation set of the model and facilitates a solution. Applying the approximate model concept, which involves replacing the mass-balance partial differential equation for a pellet with a proper ordinary differential equation, yields a substantial simplification for analysis and calculations. This approach does not require any iterative and trial and error computations [2] .

$LaNi_xAl_{1-x}O_3$ perovskites ($0<x<1$) obtained via a sol-gel related method are efficient in methane reforming (steam and dry reforming). It has been obtained solid solutions for all x values and a good homogeneity, especially if nitrate salts are used as precursors. The addition of aluminium to the $LaNiO_3$ perovskite structure generates a change in the temperature of nickel reducibility, stabilises the structure under reaction conditions, and limits the migration of the active nickel; however, stability depends on the x value. The catalyst $LaNi_{0.3}Al_{0.7}O_3$ shows good stability and ageing in steam and dry reforming over 170 h [4]. In the present work, we prepared nickel perovskite of the formula $LaNi_{0.3}Al_{0.7}O_3$ via a sol-gel method using nitrate salts and shaped it into a cylindrical pellet.

Paper first received Nov. 19, 2006, and in revised form Feb.08, 2008.
Matin Parvari, Chemical Engineering College, Iran University of Science and Technology, parvari@iust.ac.ir
Peyman Moradi, Chemical Engineering College, Iran University of Science and Technology, peyman.moradi@gmail.com

As the conversion of reactants to products is one of the most important stages in a heterogeneous reaction, we investigate kinetic models of the methane dry reforming reaction over a nickel perovskite catalyst. We conducted the reaction on a cylindrical catalyst pellet in a fixed bed reactor, and compare the results to the predictions of a mathematical model. The model is based on the mass balance of a cylindrical pellet inserted into the reactor.

2. Experimental Methodology

The $LaNi_{0.3}Al_{0.7}O_3$ was prepared in a laboratory scale via a sol-gel related method using propionic acid as a solvent and following the methods developed in [4]. Precursor solutions were prepared by individually dissolving nitrate salts of starting elements in hot propionic acid.

After dissolution into propionic acid, nickel and aluminum solutions were mixed and added a lanthanum solution, with the final solution being stirred in a reflux process until the formation of a green resin. The resulting gel was calcined under increasing temperature with a slope of 3°C/min from 25°C to 750°C and maintained at 750°C for 4 h. The catalyst powder was then shaped into a cylindrical pellet using a wet pressing method. For this stage, a paste of the catalyst powder and polyvinyl alcohol (PVA) as a binder was pressed between two punches in a hydraulic press. The catalyst pellet was then calcined at 750°C for 4 h to remove binder molecules and develop porosity.

Details of the crystalline structure of the synthesized catalyst were obtained via X-ray diffraction using a Siemens D-500 diffract meter with Cu–Kα radiation. Measurements of the specific surface area, pore volume, and pore size distribution were performed using the BET method based on the N2 physisorption capacity at 77 K on a Coulter SA 3100 pparatus.

Reactivity tests were performed on the catalyst pellet in a fixed bed reactor during the dry reforming of methane (Fig.1). Catalytic tests were performed at atmospheric pressure. The reaction conditions of the catalyst pellet were as follows: fixed bed quartz reactor (14 mm ID); feed flow rate: CH4: 38.66 ml/min, CO2 38.66 ml/min, Ar: 308.32 ml/min; number of catalyst pellets: one. The temperature program involved initial heating and two cycles. The initial heating consisted of a temperature increase from 25°C to 600°C with a gradient of 10°C/min. During this step, no significant amount of synthesis gas was produced. The first cycle comprised a continuous increase in temperature from 600°C to 800°C with a slope of 3°C/min (Ramp 1). During this stage, chromatographic analyses were performed every 50°C with a stage of 1 hr at 800°C with three Gas Chromatography analyses and a stepwise decrease every 50°C down to 600°C with GC analyses at each stage (Ramp 2). The second cycle was then performed to the same schedule as the first (Ramps 3 and 4).

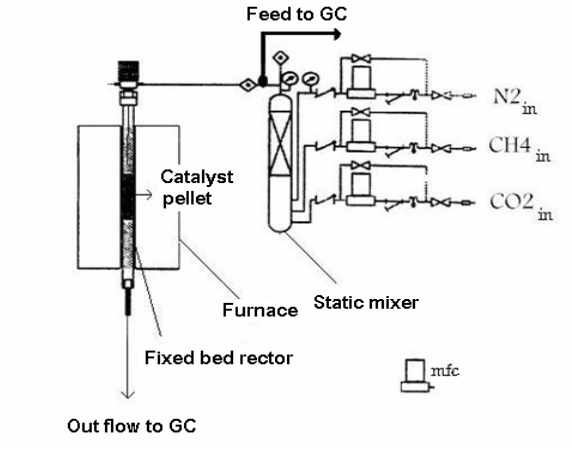

Fig. 1. Catalytic test setup

3. Theoretical Principles

3-1. Mass Transfer Theory Within The Solid

As the methane dry reforming reaction that produces syngas involves the generation of gaseous product in the porous solid, we must anticipate the potential occurrence of both molecular and Knudsen diffusion in catalyst pores. The question of whether molecular or Knudsen diffusion becomes dominant depends on the ratio of the pore diameter to the mean free path of molecular motion. If the mean free path of the molecules is greater than the diameter of the pores, intermolecular collision will be less frequent than pore wall–molecule collisions, and the diffusion coefficient for such pores will be defined by the Knudsen flow formula [6]. However, under certain reforming conditions there is such a range of pore sizes for each porous structure that both mechanisms are of vital importance and both should be considered when determining the overall diffusion coefficient. The diffusion coefficients are then effectively constants, being functions of molecular diffusion, Knudsen diffusion, the porosity of the structure, and the tortuosity factor, which is the ratio of the actual distance that a molecule travels between two points to the shortest distance between those two points [2,6,7,8]. The effective diffusion coefficient, Deff, effective bulk diffusion coefficient, Dbeff, Knudsen effective diffusion coefficient, Dkeff, and the bulk diffusion coefficient, Db, are determined respectively as follows [6,9]:

$$\frac{1}{D_{eff}} = \frac{1}{(D_b)_{eff}} + \frac{1}{(D_k)_{eff}} \tag{1}$$

$$(D_b)_{eff} = \frac{D_b \theta}{\tau} \tag{2}$$

$$(D_k)_{eff} = 9700\, \bar{r} \sqrt{\frac{T}{M}} * \frac{\theta}{\tau} \tag{3}$$

$$D_b = \frac{(0.00107 - 0.000246\sqrt{1/M_1 + 1/M_2})T^{3/2}\sqrt{1/M_1 + 1/M_2}}{P_t (r_{12})^2 f(kT/\varepsilon_{12})} \tag{4}$$

Three different diffusion models can be used, depending on the catalyst pore size. When the pore diameter (d_p) is much larger than the mean free path (λ) of diffusing molecules, diffusion takes place in the usual (Maxwellian) way, as observed outside the pores (bulk or molecular diffusion). The Knudsen number (Kn) is a dimensionless number defined as the ratio of the molecular mean free path length to a representative physical length scale. This length scale could be, for example, the radius of a body in a fluid. The number is named after Danish physicist Martin Knudsen (1871–1949). When d_p is much lower to the mean free path, the diffusing molecules encounter the pore walls more frequently than they encounter other molecules (Knudsen diffusion). In a micro-porous solid such as zeolite, reactant molecules can diffuse within pores whose diameters are close to the size of the molecules by remaining constantly in contact with the pore walls (surface or configurationally diffusion) [6].

3.2. Mechanism and Kinetics of the Reaction

In the past decade, many researchers have reported on mechanisms and kinetic models for the methane dry reforming reaction. The reaction mechanism depends on the type of catalyst used in the reaction as well as the reaction temperature and pressure [10–14]. The main stages of the reaction are as follows:

1) Dehydrogenation and conversion of methane to adsorbed arbon and hydrogen.
2) Dissociation and adsorption of carbon dioxide and hydrogen.
3) Reduction of carbon dioxide to carbon monoxide.

It has also been noted that the mechanism of dry reforming may not differ significantly from that of steam reforming. A previous study proposed that the methane dry reforming reaction involves two irreversible steps: methane and carbon dioxide dissociation, and the adsorption and surface reaction of CH_x^* and O^* free radicals [10].

Some studies use a simple power law equation ($r = K P_{CH4}^{m} P_{CO2}^{n}$) to express the rate of the methane dry reforming reaction. The lists of the parameters of the power law equation for a number of different catalysts has been collected in [10]. This kinetic model involves the participation of two active sites in the catalytic process. If the molar ratio of methane is equal to that of carbon dioxide, the partial pressure of the reactants will also be equal. In this case, the reaction rate can be expressed as follows:

$$r = KPCH\,4(m+n) \tag{5}$$

$$K = K\,0e\text{-}Ea/RT \tag{6}$$

Referring to the values of "m" and "n" for example m+n=1 for Ni/Al_2O_3 , Ru/MgO, Rh/MgO, Pd/MgO, Ir/MgO and other catalysts in [10], it is apparent that the value of m+n is close to 1 for most of the catalyst. For example In this case, a first-order equation can be considered for the reaction rate expression. Another form of the reaction rate that is useful for predicting the concentration profile in the catalyst pellet is $R_A = k''aC_A$. To evaluate the proposed model for the reaction rate, we performed catalytic tests in a micro reactor. The results are plotted in Fig.2 as $k''a$ versus temperature.

3.3. Models of Pore Diffusion

Mathematical models can be used to predict the concentration profiles of reactants within a catalyst pellet. As there is no distance between the catalyst pellet and the reactor wall, it can be assumed that all reactant molecules diffuse within the catalyst across the section of the pellet. The mass balance equation can be considered in a cylindrical element coordination (Fig. 3). The reaction rate is considered as a first-order equation. Integration of the final differential equation yields the reactant concentration profile within the catalyst pellet.

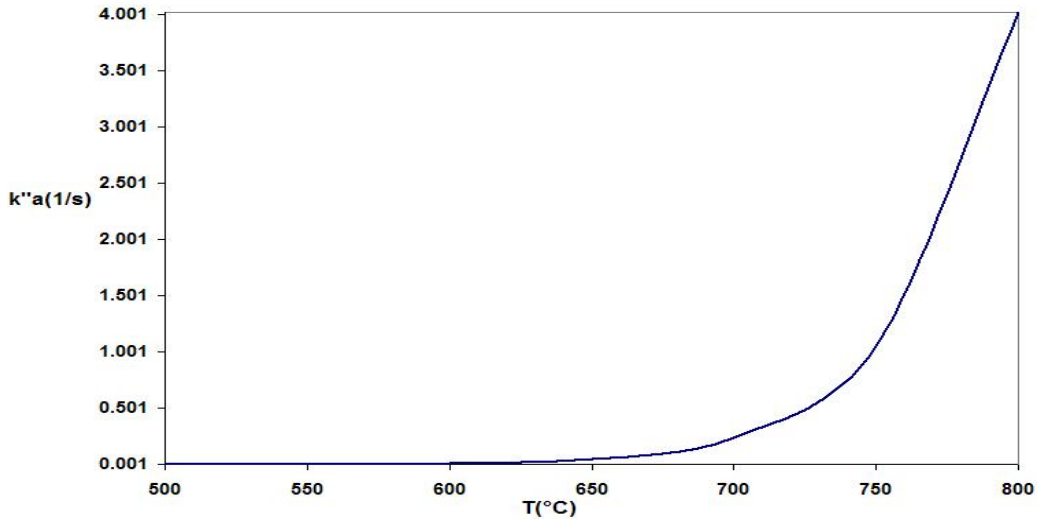

Fig 2. Kinematics data (k''a) vs. temperature

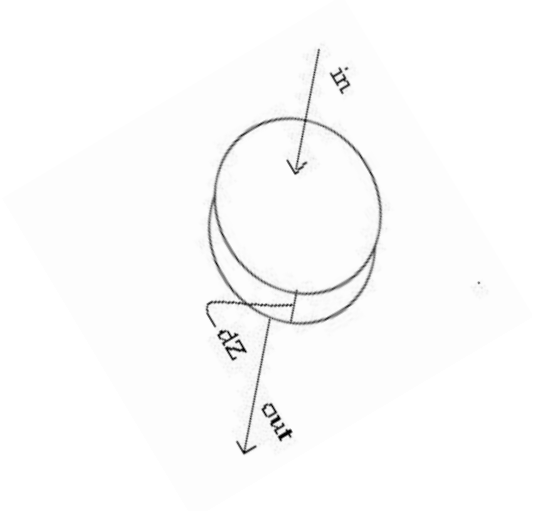

Fig 3. Coordinates for the cylindrical catalyst pellet element

The shell mass balance method and Fick's first law can be used to describe diffusion within a porous catalyst pellet. The average diffusion of the chemical species can be described in terms of an effective diffusion coefficient.

We consider a porous cylindrical catalyst element of cross-sectional area S. This particle is located in a catalytic reactor where it is submerged in a gas stream containing methane and carbon dioxide as reactants and synthesis gas as product. We presume that the concentration of methane close to the surface of the catalyst pellet is C_{AS} moles per unit volume. Species A diffuses through tortuous passages in the catalyst and is converted to the product on the catalytic surface.

We begin by calculating a mass balance for species A on a cylindrical element of thickness Z within a single catalyst particle and using $\Delta z \to 0$ gives :

$$-\frac{dN_{Az}}{dz} = R_A \tag{7}$$

Using Fick's first law and consider a situation in which species A is consumed according to a first-order chemical reaction on the catalytic surfaces Eqs. 5 and 7 become:

$$D_A \frac{d^2C_A}{dz^2} = k''aC_A \tag{8}$$

$$\frac{d^2C_A}{dz^2} - \frac{k''a}{D_A}C_A = 0 \tag{9}$$

where C_A is the concentration of Species A within the pores. The effective diffusivity D_A must be measured experimentally, and is dependant on pressure, temperature, and the catalyst pore structure. The answer of the differential equation is:

$$C_A = A\cosh\left[l\sqrt{\frac{k''a}{D_A}}(\frac{z}{l})\right] + B\sinh\left[l\sqrt{\frac{k''a}{D_A}}(\frac{z}{l})\right] \tag{10}$$

The final equation can be simplified by introducing the dimensionless parameters (Eq. 11), the Thiele modulus, Z (Eq. 12), the dimensionless length, and C, the dimensionless concentration(Eq.13):

$$\phi = l\sqrt{\frac{k''a}{D_A}} \tag{11}$$

$$Z = z/l \tag{12}$$

$$C=C_A/C_{A0} \tag{13}$$

C_{A0} is the initial concentration of species A and l is the length of the catalyst pellet.

$$C = \frac{C_A}{C_{A_0}} = \cosh(\phi Z) - \sinh(\phi Z) \tag{14}$$

The molar flux (N_{AZ}) or molar flow (W_{AZ}) at the bottom of the catalyst pellet (Z = l) is:

$$W_{AS} = S.N_{AS} = -S.C_{A0}.\frac{1}{l}.D_A\left.\frac{dC}{dZ}\right|_{Z=1} \tag{15}$$

$$\left.\frac{dC}{dZ}\right|_{Z=1} = \phi(\sinh(\phi Z) - \cosh(\phi Z)) \tag{16}$$

$$W_{AS} = -S.C_{A0}.\frac{1}{l}.D_A.\phi(\sinh(\phi) - \cosh(\phi)) \tag{17}$$

Equation 17 provides the rate of conversion (moles/sec) of reactant0 A to product B in a single catalyst pellet in terms of the relevant diffusive processes. If the catalytic surfaces are all exposed to the stream of concentration C_{AS}, then species A would not have to diffuse through the pores to an active site, and the molar rate of conversion would then be given by the product of the available surface and the surface reaction rate:

$$W_{A0} = -(S.l).(a).(-K''C_{Aout}) \tag{18}$$

$$C_{Aout} = C_{A0}.(\cosh(\phi) - \sinh(\phi)) \tag{19}$$

$$W_{A0} = (S.l).(a).(-K''C_{A0}.(\cosh(\phi) - \sinh(\phi))) \tag{20}$$

The ratio of the actual rate of reaction in the catalyst pellet (including reaction and diffusion resistance (r_{actual})) to the rate of reaction that would result if the entire interior surface were exposed to the external pellet surface concentration C_{AS} ($r_{(TS,CAS)}$) is known as the effectiveness factor ( ) [15]. Division of Eq. 17 by Eq. 20 gives:

$$\eta = \frac{r_{actual}}{r_{(T_s, C_{A_s})}} = \frac{-D_A\frac{\phi}{l}(\sinh(\phi) - \cosh(\phi))}{l * k''a * (\cosh(\phi) - \sinh(\phi))} \tag{21}$$

To express the overall rate of reaction in terms of the Thiele modulus, we combine Eqs. 15 and 21 and write the actual rate of reaction as follows:

$$N_A = \frac{-D_A \frac{\phi}{l}(\sinh(\phi) - \cosh(\phi))}{l * k'' a * (\cosh(\phi) - \sinh(\phi))} r(T_s C_{AS}) / S \quad (22)$$

4. Results Esults and Discussion

4-1. Characterization of the Formed Mixed Oxide Pellet

The XRD diagram of the $LaNi_{0.3}Al_{0.7}O_3$ mixed oxide indicates that only one perovskite phase is obtained. As indicated in a previous study [4], enlargement of the area on the XRD diagram of 2θ values between 32.7° and 33.7° shows that the main peak is located between the highest peaks of $LaNiO_3$ and $LaAlO_3$ (Fig.4a). This result indicates that a solid mixture of these two structures formed during calcination. As indicated in Fig.4b and 4c after forming the catalyst, the XRD diagram shows the same crystalline structure as the powder, indicating that no phase transformation has taken place during shaping of the powder and final calcination to remove the binders and develop porosity. Table1 provides the diffusivity factors calculated using Eqs. 1 to 3 at varying temperatures.

The BET surface area of the catalyst powder is 15.2 m^2/g. After shaping, the height and diameter of the cylindrical catalyst pellet were 15.10 mm and 13.8 mm, respectively. In the final heat treatment of the formed pellet, binder molecules were decomposed and porosity was generated with the exit of decomposed gas from the pellet.

BET surface area measurements indicate that the catalyst porosity is 42.1%, the specific surface area is $3.19*10^5$ cm^2/cm^3, and the catalyst tortuosity factor is 4 [6].

As described above, the mechanical properties of the formed pellet are affected by formation-related operating parameters such as the type and amount of binder, the applied pressure of the hydraulic press, and the conditions of the final heat treatment. The catalyst mixed oxide does not by itself possess the required mould ability and plasticity, even when the optimum water content is added: it behaves somewhat like sand. Such a powder requires a binder to produce a pellet with the desired mechanical behaviour.

Accordingly, in the formulation of the paste we used a variety of binders such as water, base oil, liquid paraffin, starch, and polyvinyl alcohol (PVA). All samples were prepared under a pressure of 800 bar and calcined at 700ºC for 4 h. The best mechanical properties of the catalyst pellet formed from water, base oil, liquid paraffin, and starch are attained with starch (0.3 kN) as a binder, with the best ratio of binder to catalyst being 0.15. The mechanical properties of pellets are vastly improved when prepared using PVA.

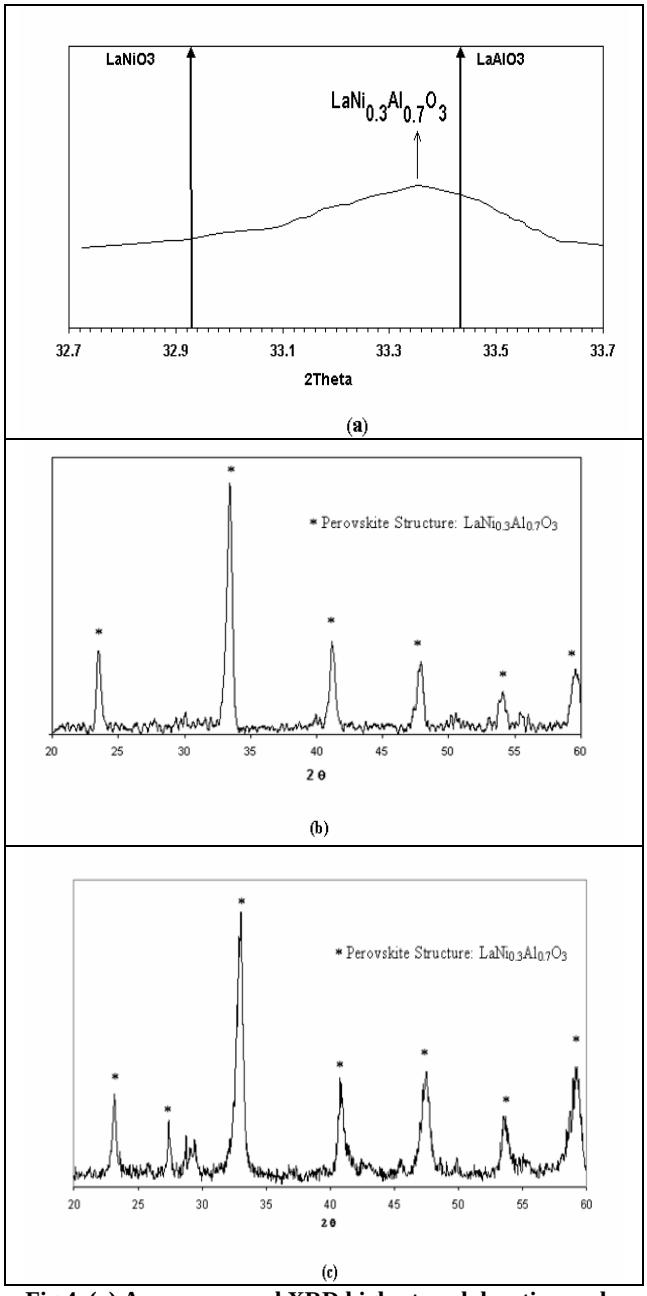

Fig 4. (a) A zoom around XRD highest peak location and compare to standard peak of LaNiO3 & LaAlO3, XRD diagram for LaNi0.3Al0.7O3 structure (b) before forming and (c) after the final heat treatment in the shaping

0.15, the pressure of the press is 800 bar, and the calcination temperature is 700°C. When the ratio of binder to catalyst is higher than 0.15, the volume of the decomposition gas is very high and small cracks propagate through the pellet, resulting in a decrease in mechanical strength.

4-2. Reactivity in Methane Dry Reforming

The dry reforming of methane was performed in a fixed bed reactor using a cylindrical catalyst pellet following a temperature program of two cycles without previous reduction. The results are presented in Figs. 5 to 8. As indicated in Fig. 5, methane is completely converted at 750°C.

Tab. 1. Diffusion factors and other data used to calculate the mass flux.

T (°C)	D_b (cm^2/s)	D_{beff} (cm^2/s)	D_{keff} (cm^2/s)	D_{eff} (cm^2/s)	Thiel Module ϕ	Effectiveness factor η_{eff}	NA (mole/cm2.s)
650	1.6060	0.169	0.00555	0.00537	4.48	0.224	3.0E-8
700	1.7382	0.183	0.00570	0.00552	9.96	0.10	2.7E-11
750	1.874	0.197	0.00584	0.00567	20.6	0.0487	6.67E-15
800	2.0130	0.212	0.00598	0.00582	39.7	0.0252	1.3E-15

A change in the catalytic behaviour is observed between the first heating and cooling ramps. During the first heating ramp, CO production begins at approximately 700°C, whereas it is still observed at the lower temperature of 600°C during the cooling ramp; this trend is related to reduction of the catalyst. Figure 6 shows that in the relationship between CO selectivity and reaction temperature. As it is indicated in this figure, CO production starts at 700°C during first ramp and it increases approximately 75%. Because of reduction of the surface, catalyst has been activated and CO production has been continued during the cooling ramp. In lower than 650°C, CO_2 production is higher than CO. Trend of the second heating ramp is similar to first ramp but CO selectivity reaches to higher than 60% at 700°C. The same phenomena has been observed for CO yield. Figure 7 shows that the CO yields are above 70% for the catalyst pellet for temperatures in excess of 700ºC.

In this case Hydrogen production starts at 700°**C** in first heating ramp and reaches to 0.8 for temperatures higher than 700ºC (Fig. 8). This is due to the oxidation of CO to H_2 when the product diffuses from active sites to the surface of the pellet**.**

4-3. Model Results

The Thiele module, ϕ, represents the ratio of reactivity to the diffusivity of the reactant species (Eq.11). As the module increases with temperature (Fig. 9), the reaction rate is higher than the diffusion rate at high temperatures. The overall rate is strongly affected by internal mass transfer and it can be affected by the reaction rate at low temperatures.

The effectiveness factor, η_{eff}, represents the ratio of the actual rate of reaction to the reaction rate at the surface conditions (Eq. 21). This factor decreases with temperature because at higher temperatures the reaction and diffusion rates increase but the rate of reaction is much higher than that of diffusion (Fig. 10). Consequently, at low temperatures the real condition is closer to the surface condition than at high temperatures.

Figure 11 shows a concentration profile for the catalyst pellet at different reaction temperatures. Because the reaction rate is proportional to the concentration of the reactants, the slope of the concentration decrease along the primary length of the catalyst pellet is greater than along the final length for all temperatures. Another point that we wish to make is that temperature affects the concentration profile. As shown in Fig. 7, an increase in temperature during the reaction results in a greater concentration drop of reactants because of an increase in the rate constant.
In comparing methane conversion and the dimensionless concentration profile predicted by the model (Figs. 12, 13) and that derived from the experiment (Fig. 5), it is apparent that the conversions from the two methods are more similar at higher temperatures (above 700°C) than at lower temperatures. For example, the conversion errors are 35% at 800°C and 45% at 650°C.

This occurs because of the assumption that the diffusion resistance in the fluid bulk is negligible. If this resistance has been considered, the conversion of methane would have been more similar to that in the experiments.

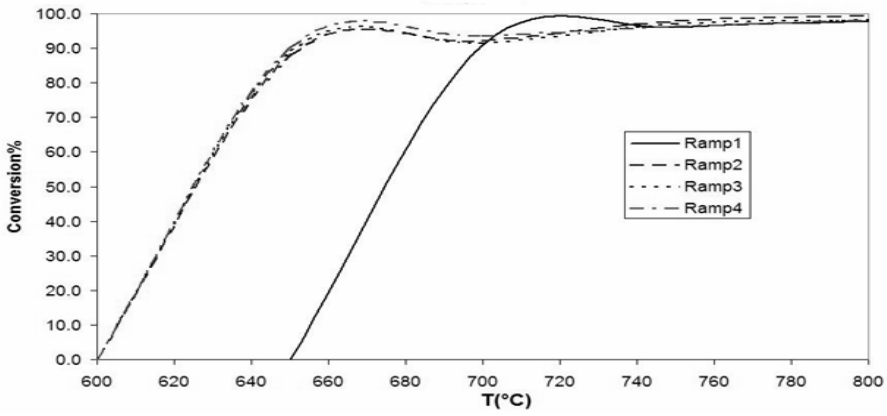

Fig 5. CH_4 conversion(%methane reacting) vs. temperature in the outlet of the fixed bed reactor when using a catalyst pellet in the dry reforming of methane.

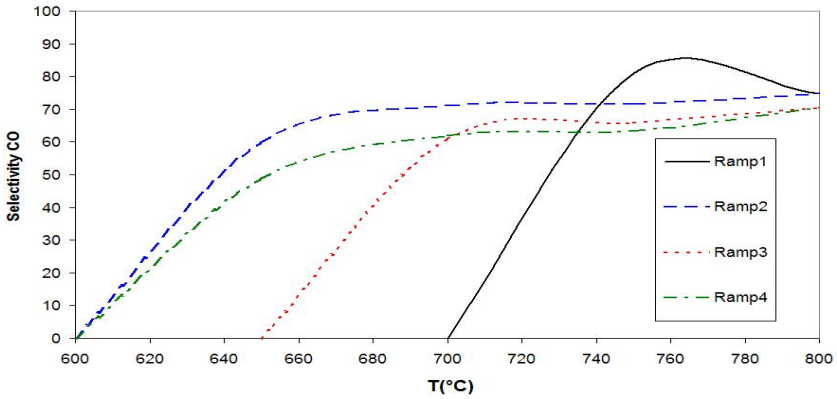

Fig 6. CO selectivity(%reacting methane converted to CO) vs. temperature in the outlet of the fixed bed reactor when using a catalyst pellet in the dry reforming of methane.

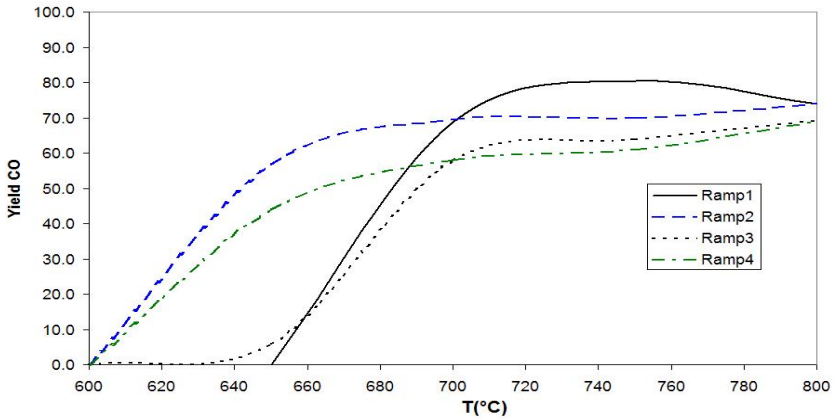

Fig 7. CO yield(%supplied methane converted to CO) vs. temperature in the outlet of the fixed bed reactor when using a catalyst pellet in the dry reforming of methane.

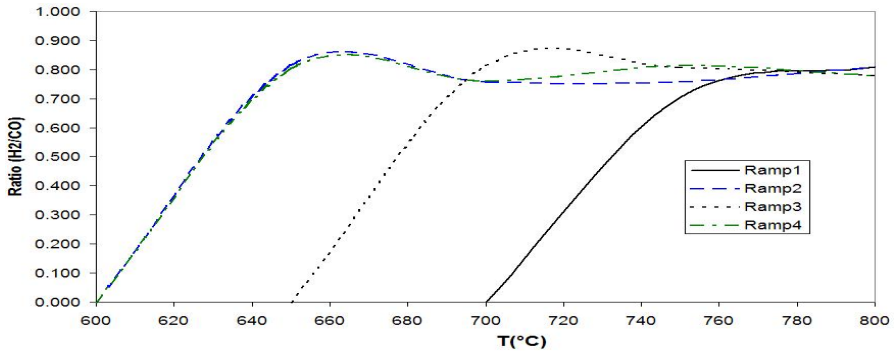

Fig 8. H_2/CO ratio vs. temperature in the outlet of the fixed bed reactor when using a catalyst pellet in the dry reforming of methane.

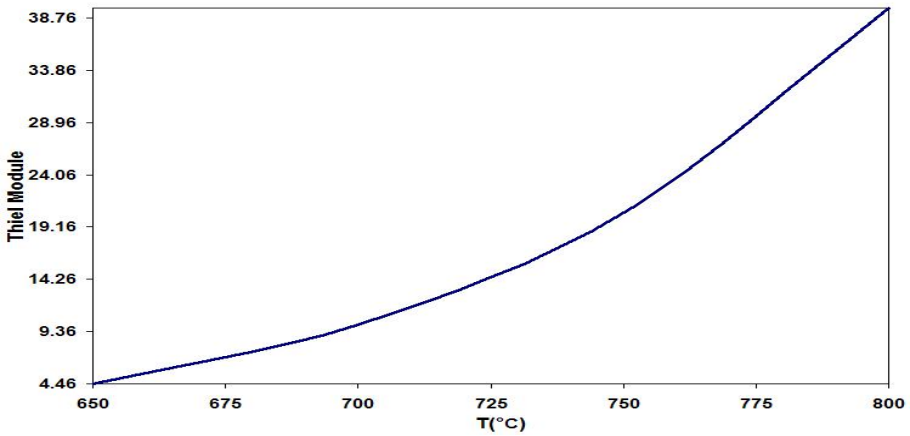

Fig 9. Thiele module vs. temperature.

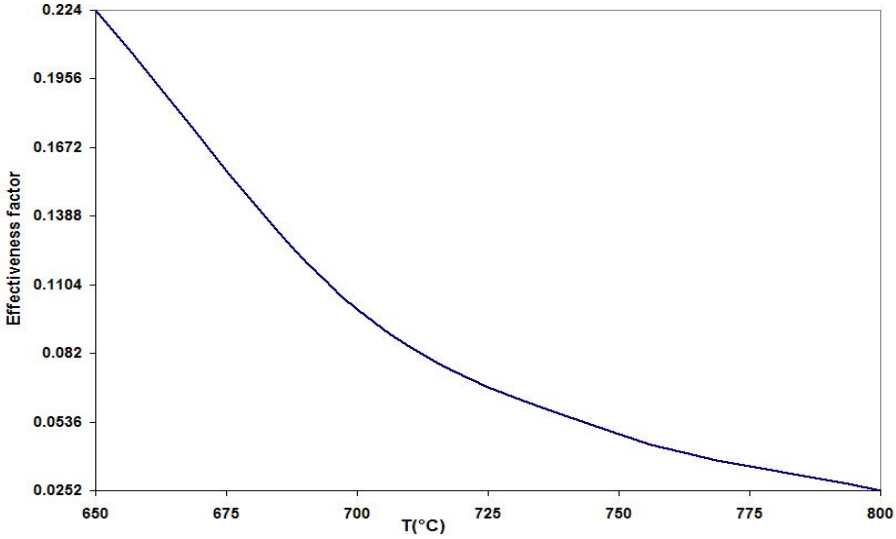

Fig 10. Effectiveness factor vs. temperature.

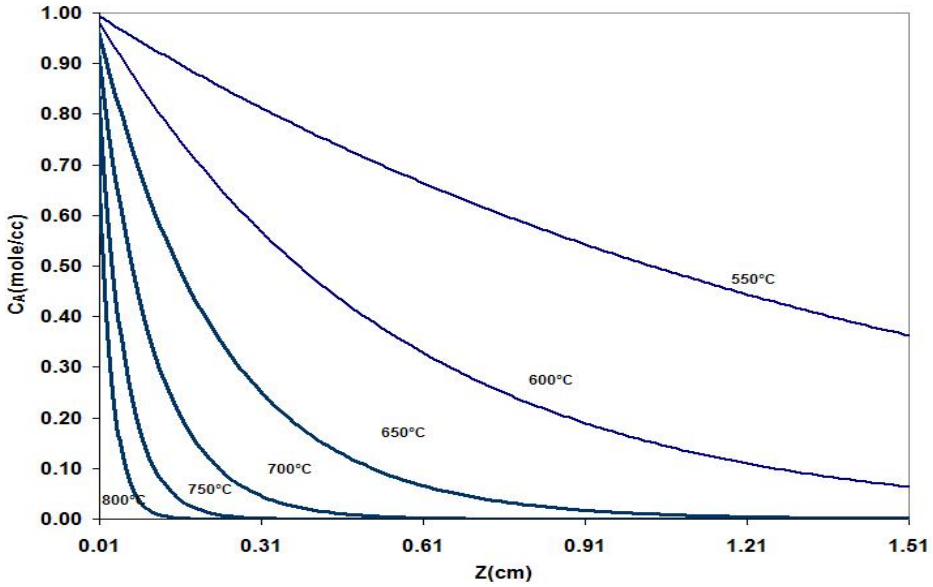

Fig 11. Concentration profile within the catalyst pellet.

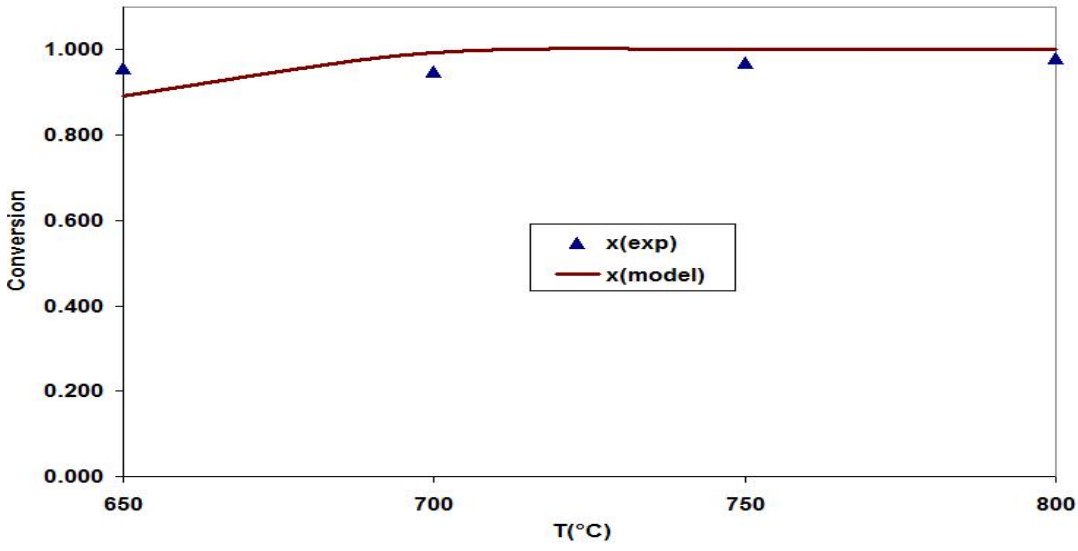

Fig 12. CH_4 conversion in the outlet of the fixed bed reactor when using a catalyst pellet and modeling results of the dry reforming of methane.

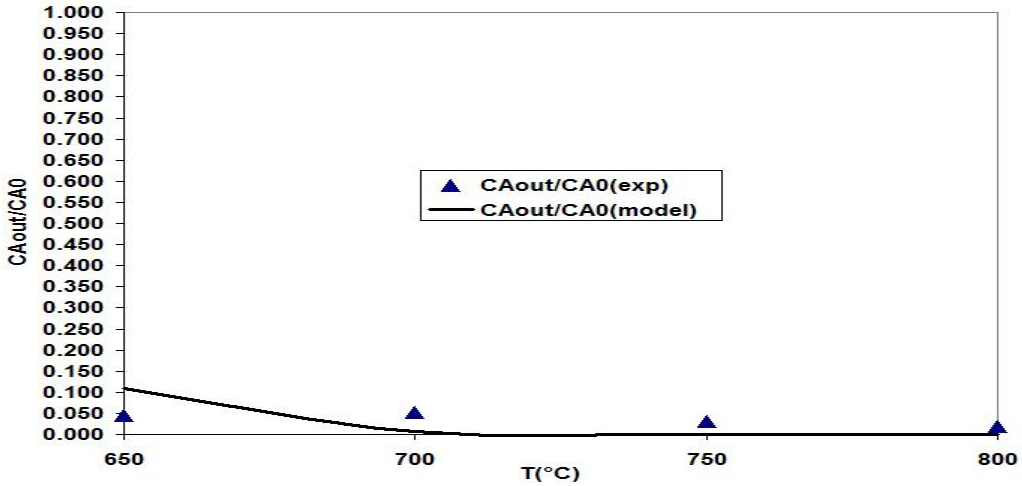

Fig 13. CH_4 conversion in the outlet of the fixed bed reactor using a catalyst pellet and modeling results of the dry reforming of methane.

5. Conclusions

The shaping process of heterogeneous catalysts is one of the most important steps in the production process of industrial catalysts. The lanthanum-nickel-aluminum perovskite was synthesized via a sol-gel method and shaped into a cylindrical form to use in the dry reforming reaction.

The Thiele module, ϕ, increases with temperature such that the reaction rate is higher than the diffusion rate at high temperatures. The overall rate is strongly affected by internal mass transfer, and is affected by the reaction rate at low temperatures. The effectiveness factor, η_{eff}, decreases with temperature because at higher temperatures the reaction and diffusion rates increase but the rate of reaction is much higher than that of diffusion. Accordingly, at low temperatures the real condition is much closer to the surface condition than at high temperatures.

Nomenclature

D_b: bulk diffusion coefficient [cm^2/s]

D_{eff}: overall diffusion coefficient [cm^2/s]

D_{keff}: Knudsen effective diffusivity [cm^2/s]

D_{beff}: effective bulk diffusion [cm^2/s]

f(kT/ε_{AB}): collision function

k: Boltzmann's constant

M, M_1, M_2: molecular mass of specified species [g/mole]

Pt: total pressure [pa]

r_{AB}: molecular separation at collision [nm]

S_g: specific surface area of the catalyst [cm^2/g]

T: temperature [K]

ε_{AB} : energy of molecular attraction = $\sqrt{\varepsilon_A \varepsilon_B}$

ρ_p : particle density [g/cm^3]

θ : internal void fraction of the solid particle [dimensionless]

τ : tortuosity factor of the pores [dimensionless]

R_A: Reaction flux[$mole/m^3.s$]

r_A: Reaction rate[mole/s]

K"a: Reaction Kinetic constant[1/s]

References

[1] Michael, C.J., Bradford, M., Albert Vannice Applied Catalysis A: General 142, 1996.

[2] Szukiewicz, M.K., AICHE, J., 46, 2000, 661.

[3] Parvari, M., Jazayeri, S.H., Taeb, A., Petit, C., Kiennemann, A., Catalysis Communication, 2, 2001, 357.

[4] Moradi, P., Parvari, M., Iranian Journal of Chemical Engineering, 3, 2006, 29.

[5] Provendier, H., Pettite, C., Estourness, C., Libs, S., Kiennemann, A., Appl. Catal. A, 180, 1999, 163.

[6] Forni, L., Catalysis Today, 52, 1999, 147.

[7] Fogler, H.S., "*Elements of Chemical Reaction engineering*", Second ed. Prentice Hall.

[8] Szukiewicz, M.K., AICHE, J., 47, 2001, 2131.

[9] Treybal, R.E., "*Mass Transfer Operations*", Third ed. McGraw-Hill, 2001.

[10] Wang, S., Lu, G.Q., *Energy & Fuels*, 10, 1996, 896.

[11] Castroluna, A., Enpromer'99, *II Congresso De Engenbaria De Processos do Mercosul*. Brasil, 1999.

[12] Joost, W.S., Gilbert, F., International Journal of Chemical Engineering, Volume1 2003, ArticleA7.

[13] Olsbye, U., Wurzel, T., Mleczko, L., Ind. Eng. Chem. Res. 36, 1997, 5180.

[14] Vaso, A., Tsipouriari, A., Xenophon, Verykios, E., catalyst.Catalysis Today 64, 2001, 83.

[15] Bird, R.B., Stewart, W.E., Lightfoot, E.N., "*Transport Phenomena*", 1960.